Vol. **127** (2015) *ACTA PHYSICA POLONICA A* No. 4

Proceedings of the 4th International Congress APMAS2014, April 24-27, 2014, Fethiye, Turkey

Morphological Changes and Enhancement of Ultraviolet Emission by Subsequent Thermal Treatment of Ga-Doped ZnO Nanostructures

U. Manzoor*
Alamoudi Water Chair, King Saud University, P.O. Box 2460, Riyadh, 11451, Saudi Arabia

ZnO nanostructures doped with a high concentration of Gallium (Ga) were synthesized on a Si substrate by thermal evaporation. Subsequent heat treatments of selected nanostructures was done at 600 °C, 700 °C, 800 °C and 900 °C. Scanning electron microscope (SEM), X-Ray diffraction (XRD) and photoluminance (PL) studies was performed after every heat treatment. Systematic scanning electron microscope (SEM) studies suggest significant sublimation at 800 °C. XRD results show that crystal quality was improved by annealing and phase separation may occur after high temperatures annealing. Ultraviolet (UV) and visible emission depends strongly on the annealing temperatures and luminescent efficiency of UV emission is enhanced significantly with heat treatment.

DOI: 10.12693/APhysPolA.127.910

PACS: 81.05.Dz, 78.55.Et

1. Introduction

Recently studies of different doped and undoped ZnO nanostructures are of great interest in the scientific community owing to their excellent optical, electrical, gas sensing and piezoelectric properties [1–4]. ZnO nanostructures have inspired scientists. Zno is also one of the most explored materials for practical applications i.e. sensors, transparent conductor oxide (TCO), photocatalysis, etc. [5, 6]. Some of these applications require high electrical conductivity, which may be achieved by replacing Zn2+ ions with ions of higher valency. For ZnO nanostructures, group III elements (Al, Ga, or In) are commonly used to substitute Zn to induce n-type conductivity [7, 8]. The success of doping is often accompanied and characterized by changes in optical, electrical, and/or structural properties of ZnO nanostructures. Despite the considerable efforts, rational synthesis of ZnO nanostructures with tunable n-type conductivity is not available. The as-synthesized ZnO nanostructures are often randomly oriented, and thus have limited applications in optoelectronic devices.

In gallium-doped zinc oxide (Ga-doped ZnO), Ga^{3+} is expected to cause a small lattice distortion (similar radii sizes of Zn and Ga) and at the same time is an efficient shallow donor in ZnO. However, Ga doping may produce $ZnGa_2O_4$ phase when the doping exceeds a certain limit. Solubility limits are reported to be close to 3 at% of Ga in ZnO [9, 10]. However, a comprehensive study is required on the effect of annealing on Ga-doped ZnO nanostructures. This will be important for high temperature applications i.e. gas sensors in which usual operating temperatures are more than 400 °C [11].

In this report, Ga-doped ZnO nanostructures were heat treated at different temperatures. Temperature dependent degradation in morphology, phase separation and optical properties were studied. Possible reasons for the improvement in optical and structural properties are discussed.

2. Experimental procedure

Ga-doped ZnO nanostructures were synthesized by vapor transport method. Equal amounts (by weight) of ZnO powder (99.0%, Hayashi Pure Chemicals Industries, Osaka, Japan) and carbon black were mixed for 4 hours in a ball mill. 0.15 g Ga_2O_3 was added to 0.6 g of the mixture, mixed using mortar and pasture (source mixture) and loaded into an alumina boat. A Silicon (Si) substrate was placed on top of alumina boat. The boat was then placed at the center of the tube furnace. Ga-doped ZnO nanostructures were synthesized at 950 °C with 15 minutes holding time. Argon (Ar) was used as carrier gas and flow rate of Ar and O_2 was 150 and 4 sccm respectively. Morphology was characterized by using scanning electron microscopy (XL30 PHILIPS Netherlands) fitted with Energy Dispersive Spectroscopy (EDX) for elemental analysis. Phase analysis of the deposited nanostructures was done by using x-ray diffraction (XRD Rigaku Tokyo, Japan). Room temperature photoluminescence of the nanostructures was measured using a custom built setup with Xenon lamp and excitation wavelength was 325 nm.

Post-synthesis heat treatment of the Ga-doped ZnO nanostructures was done at 600 °C, 700 °C, 800 °C and 900 °C for 1 hour in O_2 (99.9% pure) with a flow rate of 25 sccm. SEM, XRD and photoluminance (PL) were measured after every heat treatment.

---

*e-mail: umanzoor@ksu.edu.sa

3. Results and discussion

Figure 1a is the typical EDX area scan of Ga-doped ZnO nanostructures. The results clearly show primary and secondary peaks of Zn and Ga, suggesting that significant amount of Ga is present. A distinct Si peak is also present which may be here because of the Si substrate. A very small gold (Au) peak is also present, which is from a thin Au coating applied on Si substrate (as catalyst) before the synthesis. Figure 1b is the low magnification image of Ga-doped ZnO nanostructures. The results clearly show mixed morphologies i.e. irregular sheets of different shapes and nanowires. The size, shape and thickness of these sheets are also not consistent and it is difficult to measure the dimensions. These structures are unique in the sense that there are very few reports on mixed morphologies of Ga-doped ZnO nanostructures [12].

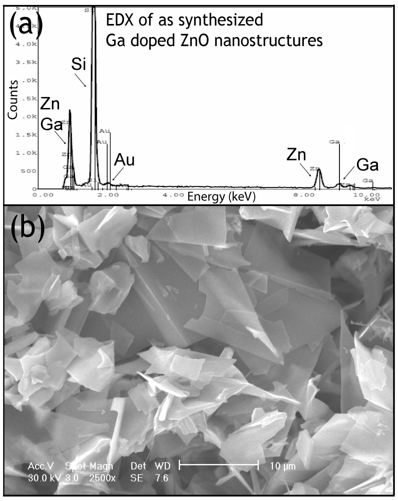

Fig. 1. EDX spectra (area scan) (a) of Ga-doped ZnO nanostructures. (b) SEM image showing mixed morphologies with mostly irregular sheet-shape structures.

Figure 2 shows SEM micrographs of a selected ZnO sheet shape structure (along with nanowires on top). There is no significant difference in morphology in the as-synthesized sheet and after heating at 600 °C and 700 °C. SEM micrographs clearly suggest a systematic degradation with temperature after annealing at 800 °C and 900 °C. Morphological changes are clearly visible at 800 °C. Significant degradation of smaller particles and substructures has started at this temperature, which may be a result of thermal etching. The size of the nanostructures play a significant role and gives a direct evidence that smaller features, having higher surface area are starting to degrade at lower temperatures than the thicker/bigger size particles. A thin film also formed on the substrate and it is expected that the ZnO sublimated from the nanostructures was deposited. After heating the same substrate at 900 °C, actual nanostructures disappeared and only nanoparticles in the form of a thin film can be seen in the SEM micrograph.

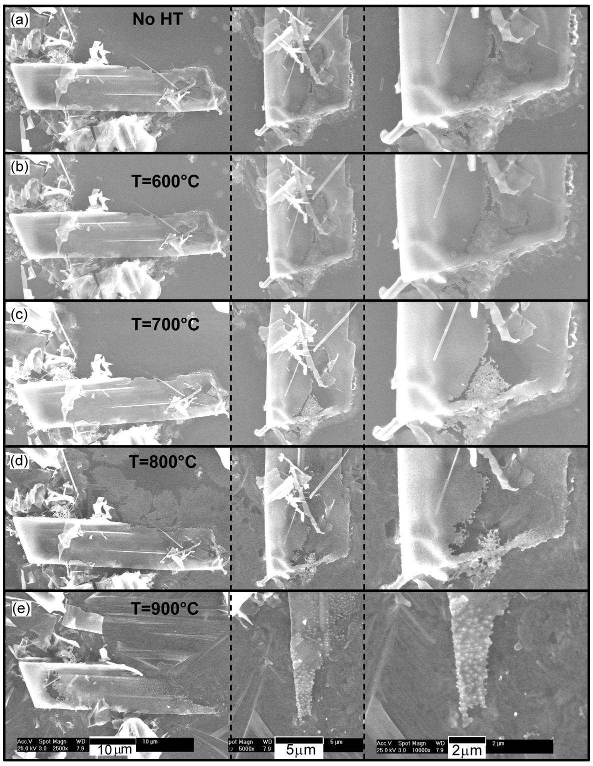

Fig. 2. SEM image (a) of sheet along with nanorods and other irregular structures (b–e) nanocomb, after subsequent heat treatments at 600 °C, 700 °C, 800 °C and 900 °C.

Zinc oxide sublimates congruently by decomposition into the gaseous elements according to the following reaction

$$\mathrm{ZnO(s)} = \mathrm{Zn(g)} + 1/2\mathrm{O_2(g)}. \tag{1}$$

During high temperature (>700 °C) annealing, the surface morphology of bulk ZnO is affected by the evaporation of lattice constituents and surface becomes rough due to the continuous evaporation [13, 14]. As the temperature further increases (900 °C), both ZnO nanostructures are completely etched out and only nanoparticles are left. Previous reports suggested that prominent sublimation in bulk ZnO occurs at 1100 °C [15]. It is interesting to note that sublimation in nanostructures occurred at 800 °C, which is much lower than the synthesis temperature (950 °C). Figure 2 gives direct evidence that ZnO nanostructures sublimate at much lower temperatures than the synthesis temperature. It may be caused by the nanosize of these structures. Also, the heat treatment was done in pure O_2 environment while nanostructures were synthesized in low O_2 environment. Therefore O_2 environment may also have a significant role in the low temperature sublimation.

XRD results (Fig. 3) clearly suggest change in (i) peak positions and (ii) full width at half-maximum (FWHM) after subsequent heat treatment. XRD results of as synthesized Ga-doped ZnO nanostructures showed very low

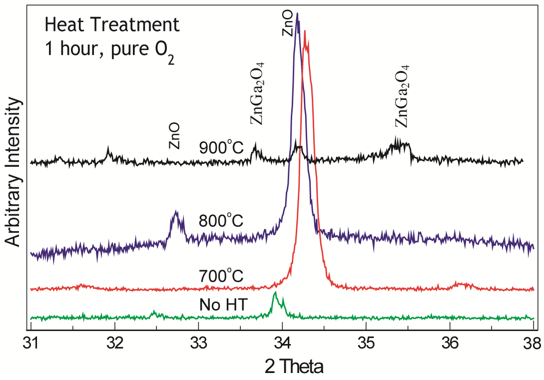

Fig. 3. Comparison of XRD results of Ga-doped ZnO nanostructures without any heat treatment and after annealing at 700 °C, 800 °C and 900 °C. XRD spectra are direct observation of narrower FWHM after annealing at 700 °C and 800 °C and some new peaks appear after annealing at 900 °C.

intensity peaks, suggesting low crystalinity and high defect density. When the same substrate was heated at 700 °C (after subsequent heat treatment at 600 °C for 1 hour; XRD data for 600 °C is not shown) there appeared a peak shift and the narrowing of FWHM. Also, only ZnO peaks are present, and no peaks of other phases appear in the graph. The shift of the peak and narrowing of the FWHM may be due to high annealing temperatures which enhance the mobility of atoms, subsequently resulting in reduced defect concentration and improve crystal quality [16]. When the same substrate was heated at 800 °C, FWHM is broader as compared to the previous heat treatment and another ZnO peak appears. This new ZnO peak may be resulted from the deposited thin film developed on the substrate as a result of sublimation (Fig. 2d). Peak shift towards lower 2θ can also result from changes in the crystal lattice due to change in defect density and phase separation of Ga atoms. Very interesting and different results are observed after annealing at 900 °C. FWHM of ZnO peaks again becomes broader, peak intensity becomes very low and new peaks of $ZnGa_2O_4$ phase appear. The angular peak position of bulk crystalline ZnO with (101) orientation is $2\theta = 34.3°$ which is comparable to JCPDS card #65-3411.

The changes in XRD patterns with subsequent heat treatments reveal some interesting findings. The as-synthesized sample initially has low crystalinity. This may be due to Ga doping and/or other crystal defects [17–19]. It is established that deep-level defects in ZnO can be recovered by annealing the material at high temperatures [20] and this fact is reflected in the XRD pattern of sample annealed at 700 °C. Point defects and other defects are mobile at these temperatures. After annealing the same sample at 800 °C, the high amount of Ga in the lattice may starts dissolution, which may be the prominent mechanism at this stage, resulting in distortion of crystal and broadening of FWHM. At 900 °C, thermal energy was enough for rejection of excess Ga and phase separation occurred. It is well-known that $ZnGa_2O_4$ is formed when ZnO and Ga are mixed together in appropriate conditions [21]. This is reflected in the XRD patterns, the peaks of $ZnGa_2O_4$ are clearly visible in the XRD patterns. In short, XRD patterns suggests that defect density decreases in the initial annealing phase (till 700 °C), then again starts to increase (800 °C), further heat treatment (900 °C) results in phase separation. There is also a low intensity peak (below 32.5°), for samples not heated and sample heated at 900 °C. These insignificant peaks may appear as a result of small quantities of other/intermediate phases because of high temperature of synthesis and the post heat treatment.

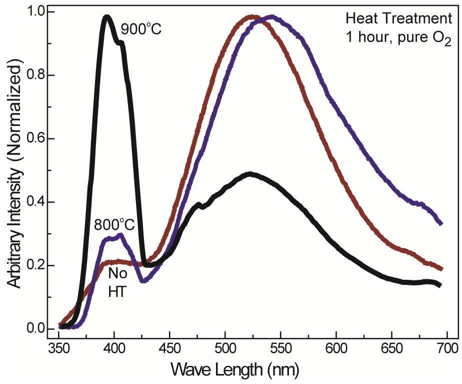

Fig. 4. PL spectra are a clear indication of increase in UV intensity with respect to green intensity after heat treatment at 800 °C. After annealing at 900 °C, NBE peak also splits into 2 peaks at 390 nm and 410 nm.

Figure 4 is the PL data of Ga-doped ZnO nanostructures. PL peaks of as-synthesized nanostructures mainly consist of a weak UV emission and a strong green emission. The UV emission, located at 400 nm, is the exciton recombination, related to near-band edge emission (NBE) of ZnO and the deep-level emission (DLE) at 525 nm usually results from the radiative recombination of a photo-generated hole with an electron occupying the oxygen vacancy and other defects [22]. Defects are often electrically active and introduce levels in the band gap of the semiconductor, which involve transitions between different charge states of the same defect [23]. Optical properties of ZnO can be tuned by annealing the samples in different environments [24]. The results suggest that UV intensity (NBE peak) significantly increases after annealing at 700 °C. DLE peak clearly splits into two peaks at 475 nm and 575 nm. These two peaks are clear indication that defect density and types have drastically changed after annealing at 700 °C, and only specific type of defects are present. Information about atomic diffusion or migration of point defects in ZnO is currently limited. Activation energies of zinc self-diffusion, in pure ZnO were reported to be in the range from 1.9 to 3.3 eV, while activation energies for oxygen self-diffusion were reported to span a much wider range, from 1.5 to 7.5 eV [25]. Doping also effects these values and interpreting these results or using them in a predictive manner is not straightforward. After annealing the same sample at 800 °C, there is a blue shift of NBE peak and peak intensities of DLE peaks decrease. Point defects i.e. oxygen vacancy, oxygen interstitial, zinc vacancy, and impurities are considered to be possible cause for these bands [26]. It is well known that DLE related defects cannot be completely removed by annealing and, on the contrary, the annealing conditions actually favor their formation. Point defects at compound semiconductor surfaces are, for entropy reasons, thermodynamically stable at high temperatures [27]. Therefore it is difficult to remove completely the point defects only by thermal treatment in Ga-doped ZnO nanostructures and a minor peak may always present in the PL data.

When the same sample was annealed at 900 °C, there was again a drastic change in the PL spectra (as in XRD, Fig. 3). NBE peak splits into 2 very distinct peaks at 390 nm and 410 nm. DLE peaks didn't show significant shift but their relative intensity decreased significantly. The phenomena of NBE peak splitting can be explained by comparing XRD results in which peaks of other phase are clearly visible. It is expected that $ZnGa_2O_4$ is precipitated out as separate phase. The two separate peaks in the UV range can be from the 2 distinct phases appeared after annealing at 900 °C.

XRD results and PL data are in perfect agreement with each other. The increase in UV and XRD intensities suggests decrease in the crystal defects quantity and improvement of the quality of ZnO. XRD peak shift also indicates an improvement in the overall crystal structure. Hence it can be suggested that high annealing temperatures (upto 800 °C) provide enough energy to enhance mobility and diffusion/rejection, that could decrease the number of defects and improve overall crystal quality [28]. However, when Ga-doped ZnO nanostructures were annealed at 900 °C phase separation occurs and new peaks appear in XRD and PL data.

Acknowledgments

This project was supported by NSTIP strategic technologies program number (12-WAT-2451-02) in the Kingdom of Saudi Arabia.

This project was also funded by the National Plan for Science, Technology and Innovation (MAARIFAH), King Abdulaziz City for Science and Technology, Kingdom of Saudi Arabia, Award Number (2451).

References

[1] M. Law, J. Goldberger, P. Yang, *Annu. Rev. Mater. Res.* **34**, 83 (2004).

[2] Kolmakov, M. Moskovits, *Annu. Rev. Mater. Res.* **34**, 151 (2004).

[3] Z. Chen, N. Wu, Z. Shan, M. Zhao, S. Li, C.B. Jiang, M.K. Chyu, S.X. Mao, *Scripta Mater.* **52**, 63 (2005).

[4] Y.S. No, H.Y. Yang, J.Y. Kim, T.W. Kim, *J. Ceram. Process. Res.* **14**, 284 (2013).

[5] Y. Wu, H. Yan, M. Huang, B. Messer, J.H. Song, P. Yang, *Chem. Eur. J.* **8**, 1260 (2002).

[6] L. Zhi-Min, Z. Hong-Zhou, X. Jun, Y. Da-Peng, *Chin. Phys. Lett.* **22**, 987 (2005).

[7] Z.W. Pan, S.M. Mahurin, S. Dai, D.H. Lowndes, *Nano Lett.* **5**, 723 (2005).

[8] S.-H. Yu, J. Yang, Y.-T. Qian, M. Yoshimura, *Chem. Phys. Lett.* **361**, 362 (2002).

[9] Y.H. Leung, A.B. Djurisic, J. Gao, M.H. Xie, Z.F. Wei, S.J. Xu, W.K. Chan, *Chem. Phys. Lett.* **394**, 452 (2004).

[10] M. Amin, U. Manzoor, M. Islam, A. Bhatti, N. Shah, *Sensors* **12**, 13842 (2012).

[11] L.L. Liew, H.Q. Le, G.K.L. Goh, *Mater. Res. Innov.* **15**, 357 (2011).

[12] J.-H. Park, Y.-J. Choi, J.-G. Park, *J. Cryst. Growth* **280**, 161 (2005).

[13] U. Manzoor, D.K. Kim, *Physica E* **41**, 500 (2009).

[14] Z.L. Wang, X.Y. Kong, J.M. Zuo, *Phys. Rev. Lett.* **91**, 185502 (2003).

[15] C. Ma, D. Moore, J. Li, Z.L. Wang, *Adv. Mater.* **15**, 228 (2003).

[16] A.B. Djurisic, X. Chen, Y.H. Leung, A.M. Ching Ng, *J. Mat. Chem.* **22**, 6526 (2012).

[17] Z.L. Wang, *J. Phys: Condens. Matter.* **16**, R829 (2004).

[18] U. Manzoor, D.K. Kim, *Scripta Mater.* **54**, 807 (2006).

[19] D. Kohl, M. Henzler, G. Heiland, *Surf. Sci.* **41**, 403 (1974).

[20] M. Grunze, W. Hirschwald, D. Hofmann, *J. Cryst. Growth* **52**, 241 (1981).

[21] H. Iwanaga, T Yoshiie, T. Yamaguchi, N. Shibata, *J. Cryst. Growth* **47**, 703 (1979).

[22] K. Vanheusden, W.L. Warren, C.H. Seager, D.R. Tallant, J.A. Voigt, B.E. Gnade, *J. Appl. Phys.* **79**, 7983 (1996).

[23] D.C. Reynolds, D.C. Look, B. Jogai, *J. Appl. Phys.* **89**, 6189 (2001).

[24] W. Gopel, *J. Vac. Sci. Technol.* **16**, 1229 (1979).

[25] J. Lim, K. Shin, H.W. Kim, C. Lee, *Mater. Sci. Eng. B* **107**, 301 (2004).

[26] B. Lin, Z. Fu, Y. Jia, *Appl. Phys. Lett.* **79**, 943 (2001).

[27] H.-J. Ko, T. Yao, Y. Chen, S.-K. Hong, *J. Appl. Phys.* **92**, 4354 (2002).

[28] Y. Zhang, G. Du, X. Yang, B. Zhao, Y. Ma, T. Yang, H.C. Ong, D. Liu, S. Yang, *Semicond. Sci. Techn.* **19**, 755 (2004).